Dynamic Stability of a Nonrigid Parachute and Payload System

DEAN WOLF*
Northrop Corporation, Newbury Park, Calif.

The three-dimensional motion of a nonrigid parachute and payload system is studied. Both the parachute and payload are assumed to have five degrees-of-freedom (roll about the axes of symmetry is neglected). They are coupled together by a fixed-length connector, or riser. The general nonlinear equations of motion are put in a form that is convenient for digital computer solutions. All equations are written in dimensionless form and, using small-disturbance theory, are linearized. The linear equations are then examined in a stability analysis. A proposed method of checking the linear stability criterion by forming the general solution of the linear equations is discussed. A sample stability analysis is presented to show how the methods developed might be applied to a particular problem. The problem consists of selecting a parachute to stabilize a statically unstable payload. With the methods developed, it is possible to examine in considerable detail the dynamic behavior of a nonrigid parachute and payload system.

Nomenclature

A = reference area
B_m, B_i = apparent inertia coefficients
$B_{ik}{}^j$ = direction cosine (i,j,k = 1–3)
B_{Rj}, B_{Sj} = direction cosine products
C = velocity magnitude
c = dimensionless velocity magnitude
C_I = moment of inertia coefficient
C_N, C_T = force coefficients
$C_{N\alpha}, C_{T\alpha}$ = force coefficient slopes
C_{T_2} = dimensionless riser force
D = reference diameter
D_* = dimensionless time derivative
F = steady aerodynamic force
F_2 = riser force
Fr = Froude number
F_x, F_y, F_z = x,y,z force components
G_1–G_{15} = parameters in small-disturbance analysis
g = gravitational acceleration
I = moment of inertia
I_a = apparent moment of inertia
i = dimensionless moment of inertia
k = dimensionless mass
L = length
m = mass
m_a = apparent mass
P_j, Q_j = angular velocities
p_j, q_j = dimensionless angular velocities
U_j, V_j = velocity components
W_j
u_j, v_j, w_j = dimensionless velocities
x_j, y_j, z_j = body-axis coordinates
x_e, y_e, z_e = Earth-fixed coordinates
α = angle of attack
ρ = fluid density
λ = root of characteristic polynomial
λ_p = most positive root real part
ψ_j, θ_j, ϕ_j = Euler angles

Superscript

j = free superscript (j = 1–3)

Subscripts

0 = reference descent condition
1 = parachute or parachute body axis
2 = riser or riser body axis
3 = payload or payload body axis
j = free subscript (j = 1–3)

Presented as Paper 70-209 at the AIAA 8th Aerospace Sciences Meeting, New York, January 19–21, 1970; submitted February 26, 1970; revision received September 28, 1970.

* Member of the Research Group. Associate Member AIAA.

Introduction

THE rapid increase in the use of parachutes during the past decade has far outpaced the development of basic technologies necessary for efficient parachute design. More demanding lower atmospheric uses combined with uses in space and ocean related sciences have confronted the parachute designer with a broad range of poorly understood phenomena.

Early studies of parachute dynamics were conducted by Henn[1] and Brown[2] for small-amplitude planar motion. Lester[3] made certain corrections to these studies by carefully discussing the way in which apparent (hydrodynamic) inertia effects are included in the equations of motion. The first stability criterion for small-amplitude planar motion was presented by Heinrich and Rust.[4] Ludwig and Heins[5] solved the equations of motion for large-amplitude planar motion using a digital computer.

Three-dimensional parachute motions were first studied by White and Wolf.[6] Both a small-disturbance stability criterion and digital computer solutions of the equations of motion were used.

All of the preceding studies assumed a rigid parachute with a neutral payload. Payload aerodynamic forces were included by Heinrich and Rust[7] for planar motion of a rigid system. Nonrigid effects have been included in the equations for planar motion by Neustadt et al.[8]

The primary purpose of this investigation is to develop the methods required to study the stability and the three-dimensional motion of a nonrigid parachute and payload system. Because of the cumbersome nature of a problem of this type, the analysis is tailored for extensive use of a digital computer.

Equations of Motion

The parachute and payload are represented in this study by a lumped-parameter model. The equations of motion are therefore ordinary differential equations. Since large amplitude motions are allowed, the equations are also nonlinear. Numerical solutions to equations of this type are well within the capabilities of modern digital computers.

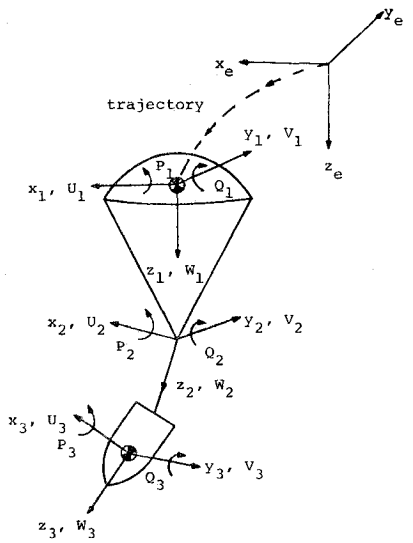

Fig. 1 Coordinate systems.

Simplifying Assumptions

In order to reduce the problem to one of an appropriate size, a number of simplifying assumptions have been made. 1) The parachute and payload are each rigid, axisymmetric bodies. 2) They are connected by a fixed-length connector, or riser, attached along the axes of symmetry. 3) Five degrees-of-freedom are allowed for each body, with roll about the axes of symmetry being ignored. 4) Steady aerodynamic forces on the parachute and payload are assumed to be functions only of instantaneous angles of attack (see Figs. 2 and 3). 5) The centers of pressure for steady aerodynamic forces are taken to be points along the respective axes of symmetry. 6) Unsteady fluid effects for the parachute are represented by scalar values of apparent mass and moment of inertia. 7) The center of parachute apparent mass is coincident with parachute center of mass. 8) Unsteady fluid effects for the payload are ignored. 9) Forebody wake effects are ignored. 10) A flat Earth with no winds is assumed for trajectory calculations. The model describes the motion of two dynamically coupled rigid bodies upon which simplified aerodynamic forces act.

Coordinate Systems

The motion of a body in space can be described by the motion of a set of coordinate axes attached to the body with respect to a reference axis system. Body axes attached to the parachute, riser, and payload are used to describe an arbitrary motion of these components in an Earth-fixed system (x_e,y_e,z_e). In all three body-axis systems (x_j,y_j,z_j) there are linear velocities (U_j,V_j,W_j) and angular velocities (P_j,Q_j), with j taking on values of 1–3 as illustrated in Fig. 1. All axis systems are right-handed orthogonal systems.

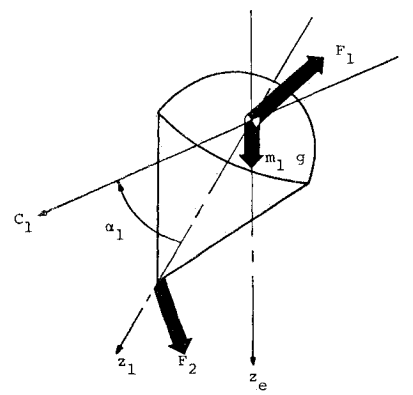

Fig. 2 Forces on parachute.

The Earth-fixed axes are aligned with any body-axis system by a series of three Euler angle rotations in the following order: ψ_j = a rotation about z_j; θ_j = a rotation about y_j after ψ_j; and ϕ_j = a rotation about x_j after ψ_j and θ_j. Velocities of the three axis systems are expressed in Earth-fixed coordinates as follows:

$$\begin{aligned}(dx_e/dt)_j &= U_jB_{11}{}^j + V_jB_{12}{}^j + W_jB_{13}{}^j\\ (dy_e/dt)_j &= U_jB_{21}{}^j + V_jB_{22}{}^j + W_jB_{23}{}^j\\ (dz_e/dt)_j &= U_jB_{31}{}^j + V_jB_{32}{}^j + W_jB_{33}{}^j\end{aligned} \tag{1}$$

where direction cosines are functions of the Euler angles;

$$\begin{aligned}B_{11}{}^j &= \cos\theta_j\cos\psi_j\\ B_{12}{}^j &= \sin\phi_j\sin\theta_j\cos\psi_j - \cos\phi_j\sin\psi_j\\ B_{13}{}^j &= \cos\phi_j\sin\theta_j\cos\psi_j + \sin\phi_j\sin\psi_j\\ B_{21}{}^j &= \cos\theta_j\sin\psi_j\\ B_{22}{}^j &= \sin\phi_j\sin\theta_j\sin\psi_j + \cos\phi_j\cos\psi_j\\ B_{23}{}^j &= \cos\phi_j\sin\theta_j\sin\psi_j - \sin\phi_j\cos\psi_j\\ B_{31}{}^j &= -\sin\theta_j\\ B_{32}{}^j &= \sin\phi_j\cos\theta_j\\ B_{33}{}^j &= \cos\phi_j\cos\theta_j\end{aligned} \tag{2}$$

Euler angle time derivatives are expressed in terms of angular velocities and Euler angles in the following way:

$$\begin{aligned}d\psi_j/dt &= Q_j\sin\phi_j\sec\theta_j,\ d\theta_j/dt = Q_j\cos\phi_j\\ d\phi_j/dt &= P_j + Q_j\sin\phi_j\tan\theta_j\end{aligned} \tag{3}$$

By integrating Eqs. (1) and (3) one obtains the position and angular orientation of the three axis systems as a function of time. The appropriate linear and angular velocities required are supplied by the equations of motion.

General Equations

By using straightforward physical arguments, the equations of motion derived by Etkin[9] are modified to describe the two-body system. First, the two-body system is divided into two separate rigid bodies. The rigid-body equations are then modified appropriately to apply to the parachute and payload. Next, constraint equations are written, which again couple the two bodies. Finally, the complete system of equations is put in a form convenient for solution on a digital computer.

Figure 2 illustrates the parachute portion of the system. The five force and moment equations for the parachute become

$$F_{1x} + m_1gB_{31}{}^1 + F_2B_{R1} = (m_1 + m_a)(dU_1/dt + Q_1W_1) \tag{4a}$$

$$F_{1y} + m_1gB_{32}{}^1 + F_2B_{R2} = (m_1 + m_a)(dV_1/dt - P_1W_1) \tag{4b}$$

$$F_{1z} + m_1gB_{33}{}^1 + F_2B_{R3} = (m_1 + m_a)\times(dW_1/dt + P_1V_1 - Q_1U_1) \tag{4c}$$

$$-F_2L_1B_{R2} = (I_1 + I_a)dP_1/dt \tag{4d}$$

$$F_2L_1B_{R1} = (I_1 + I_a)dQ_1/dt \tag{4e}$$

Direction cosine products are defined by

$$B_{Rj} = B_{1j}{}^1B_{13}{}^2 + B_{2j}{}^1B_{23}{}^2 + B_{3j}{}^1B_{33}{}^2 \tag{5}$$

They provide a convenient way of breaking the riser force into components in the parachute body-axis system.

The payload portion of the system is shown in a similar form in Fig. 3. Five more force and moment equations are

needed to describe the payload;

$$F_{3x} + m_3 g B_{31}^{3} - F_2 B_{S1} = m_3(dU_3/dt + Q_3 W_3) \quad (6a)$$

$$F_{3y} + m_3 g B_{32}^{3} - F_2 B_{S2} = m_3(dV_3/dt - P_3 W_3) \quad (6b)$$

$$F_{3z} + m_3 g B_{33}^{3} - F_2 B_{S3} = m_3(dW_3/dt + P_3 V_3 - Q_3 U_3) \quad (6c)$$

$$-F_2 L_3 B_{S2} - F_{3y} L_4 = I_3 \frac{dP_3}{dt} \quad (6d)$$

$$F_2 L_3 B_{S1} + F_{3x} L_4 = I_3 \frac{dQ_3}{dt} \quad (6e)$$

System dimensions are illustrated in Fig. 4. Again, riser force components are obtained with direction cosine products defined by

$$B_{Sj} = B_{1j}^{3} B_{13}^{2} + B_{2j}^{3} B_{23}^{2} + B_{3j}^{3} B_{33}^{2} \quad (7)$$

Coupling Equations

The equations are not yet complete. Riser force and direction cosines in the riser coordinate system appear in all equations of motion. They are provided by the constraint or coupling equations.

The riser attachment points on the parachute and payload must remain a fixed distance apart. The constraint is written in terms of velocities, since velocities are used as dependent variables.

If velocity components in adjacent coordinate systems are equated at both ends of the riser, two sets of three equations are obtained. Riser linear velocity components are eliminated and one set of three equations is obtained in the following form:

$$B_{j1}^{2} L_2 Q_2 - B_{j2}^{2} L_2 P_2 = B_{j1}^{3}(U_3 - L_3 Q_3) + B_{j2}^{3}(V_3 + L_3 P_3) + B_{j3}^{3} W_3 - B_{j1}^{1}(U_1 + L_1 Q_1) - B_{j2}^{1}(V_1 - L_1 P_1) - B_{j3}^{1} W_1 \quad (8)$$

Equations (3, 4, 6, and 8) provide 22 independent relations between the 22 variables $(U_1,V_1,W_1,U_3,V_3,W_3,P_j,Q_j,\psi_j,\theta_j,\phi_j,F_2)$ if Eqs. (2, 5, and 7) are substituted appropriately, and aerodynamic forces are expressed as functions of velocity components. Unfortunately, the form of these relations is not convenient for a numerical solution. First derivatives of the riser force and riser angular velocities do not appear, so a straightforward numerical integration is not possible.

With a significant increase in complexity, it is possible to differentiate Eq. (8). The resulting equations are solved for dQ_2/dt, dP_2/dt and dW_1/dt with $j = 1,2$, and 3, respectively;

$$L_2\left(Q_2 B_{j3}^{2} + P_2 B_{j3}^{2} - B_{j1}^{2}\frac{dQ_2}{dt} + B_{j2}^{2}\frac{dP_2}{dt}\right) = B_{j3}^{3} Q_3(U_3 - L_3 Q_3) - B_{j3}^{3} P_3(V_3 + L_3 P_3) - W_3(B_{j1}^{3} Q_3 - B_{j2}^{3} P_3) - B_{j3}^{1} Q_1(U_1 + L_1 Q_1) + B_{j3}^{1} P_1(V_1 - L_1 P_1) + W_1(B_{j1}^{1} Q_1 - B_{j2}^{1} P_1) - B_{j1}^{3}\left(\frac{dU_3}{dt} - L_3\frac{dQ_3}{dt}\right) - B_{j2}^{3}\left(\frac{dV_3}{dt} + L_3\frac{dP_3}{dt}\right) - B_{j3}^{3}\frac{dW_3}{dt} - B_{j1}^{1}\left(\frac{dU_1}{dt} + L_1\frac{dQ_1}{dt}\right) + B_{j2}^{1}\left(\frac{dV_1}{dt} - L_1\frac{dP_1}{dt}\right) + B_{j3}^{1}\frac{dW_1}{dt} \quad (9)$$

With $j = 3$, Eq. (9) contains a strong hint of what to do with the unknown riser force. With the derivative dW_1/dt given by this equation, Eq. (4c) can be solved to give the riser force;

$$F_2 = 1/B_{R3}[(m_1 + m_a)(dW_1/dt + P_1 V_1 - Q_1 U_1) - F_{1z} - m_1 g B_{33}^{1}] \quad (10)$$

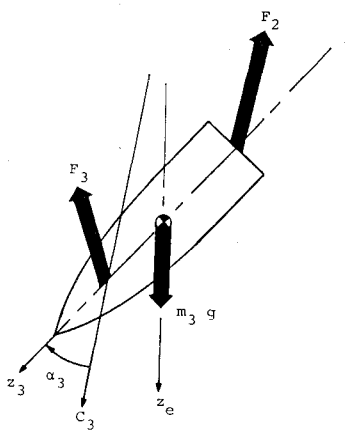

Fig. 3 Forces on payload.

Equations (3, 4a, 4b, 4d, 4e, 6, and 9) now provide 21 first-order ordinary differential equations in the 21 variables $(U_1,V_1, W_1,U_3,V_3,W_3,P_j,Q_j,\psi_j,\theta_j,\phi_j)$ when Eqs. (2,5,7, and 10) are substituted appropriately. The form of the 21 equations allows a straightforward numerical solution.

Nondimensional Equations

For a general study of this type, dimensionless equations are much more convenient to work with than their dimensional counterparts. All variables are put in nondimensional form using the system length L and the steady glide speed C_0 (see Fig. 4). Sample nondimensional variables are defined as follows:

$$u_1 = U_1/C_0;\ p_j = LP_j/C_0;\ t_* = C_0 t/L \quad (11)$$

Substituting the nondimensional variables into Eqs. (4) and (6), the equations of motion are put in the following dimensionless form:

$$\frac{du_1}{dt_*} = -\frac{C_{N1} c_1^{2} u_1}{k_1 r_1 (c_1^{2} - w_1^{2})^{1/2}} + \frac{r_{1g} C_{T0} B_{31}^{1}}{k_1 r_1} + \frac{C_{T2} c_1^{2} B_{R1}}{k_1 r_1} - q_1 w_1 \quad (12a)$$

$$\frac{dv_1}{dt_*} = -\frac{C_{N1} c_1^{2} v_1}{k_1 r_1 (c_1^{2} - w_1^{2})^{1/2}} + \frac{r_{1g} C_{T0} B_{32}^{1}}{k_1 r_1} + \frac{C_{T2} c_1^{2} B_{R2}}{k_1 r_1} + p_1 w_1 \quad (12b)$$

$$dp_1/dt_* = -C_{T2} c_1^{2} B_{R2}/i_1 r_1^{2} \quad (12c)$$

$$dq_1/dt_* = C_{T2} c_1^{2} B_{R1}/i_1 r_1^{2} \quad (12d)$$

$$\frac{du_3}{dt_*} = -\frac{C_{N3} c_3^{2}(u_3 + r_4 q_3)}{k_3 r_3 (c_3^{2} - w_3^{2})^{1/2}} + \frac{r_{3g} C_{T0} B_{31}^{3}}{k_3 r_3 r_A} - \frac{C_{T2} c_1^{2} B_{S1}}{k_3 r_3 r_A} - q_3 w_3 \quad (12e)$$

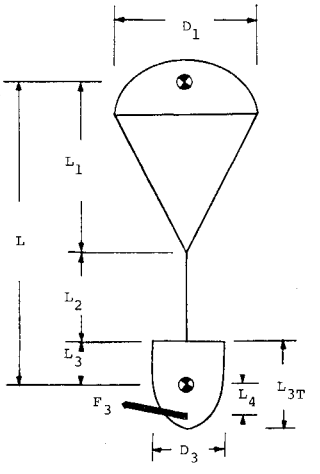

Fig. 4 System dimensions.

$$\frac{dv_3}{dt_*} = -\frac{C_{N3}c_3^2(v_3 - r_4p_3)}{k_3r_3(c_3^2 - w_3^2)^{1/2}} + \frac{r_{3g}C_{T0}B_{32}^3}{k_3r_3r_A} - \frac{C_{T2}c_1^2B_{S2}}{k_3r_3r_A} + q_3w_3 \tag{12f}$$

$$\frac{dw_3}{dt_*} = -\frac{C_{T3}c_3^2}{k_3r_3} + \frac{r_{3g}C_{T0}B_{33}^3}{k_3r_3r_A} - \frac{C_{T2}c_1^2B_{S3}}{k_3r_3r_A} - p_3v_3 + q_3u_3 \tag{12g}$$

$$\frac{dp_3}{dt_*} = -\frac{C_{T2}c_1^2B_{S2}}{i_3r_3^2r_A} + \frac{C_{N3}c_3^2(v_3 - r_4p_3)r_4}{i_3r_3^3(c_3^2 - w_3^2)^{1/2}} \tag{12h}$$

$$\frac{dq_3}{dt_*} = \frac{C_{T2}c_1^2B_{S1}}{[i_3r_3^2r_A} - \frac{C_{N3}c_3^2(u_3 + r_4q_3)r_4}{i_3r_3^3(c_3^2 - w_3^2)^{1/2}} \tag{12i}$$

The riser force is written in dimensionless coefficient form as

$$C_{T2} = \frac{1}{B_{R3}}\left[\left(\frac{dw_1}{dt_*} + p_1v_1 - q_1u_1\right)\frac{k_1r_1}{c_1^2} + C_{T1} - \frac{r_{1g}C_{T0}B_{33}^1}{c_1^2}\right] \tag{13}$$

Euler angle derivatives of Eqs. (3) are put in nondimensional form by substituting dimensionless angular velocities p_j and q_j. Also, the lengthy Eq. (9) is put in nondimensional form quite simply by inserting dimensionless linear and angular velocities $(u_1,v_1,w_1,u_3,v_3,w_3,p_j,q_j)$ and by replacing all lengths (L_1,L_2,L_3) by length ratios (r_1,r_2,r_3).

A formidable collection of dimensionless parameters has been introduced into the equations. They are defined as follows:

$$\begin{gathered} k_1 = \frac{2(m_1 + m_a)}{\rho A_1L_1};\quad k_3 = \frac{2m_3}{\rho A_3L_3};\quad i_1 = \frac{2(I_1 + I_a)}{\rho A_1L_1^3} \\ i_3 = \frac{2I_3}{\rho A_3L_3^3};\quad r_{1g} = \frac{m_1}{m_1 + m_3};\quad r_{3g} = \frac{m_3}{m_1 + m_3} \\ C_{T0} = \frac{(m_1 + m_3)g}{\frac{1}{2}\rho C_0^2A_1};\quad r_A = \frac{A_3}{A_1};\quad r_1 = \frac{L_1}{L}; \\ r_2 = \frac{L_2}{L};\quad r_3 = \frac{L_3}{L};\quad r_4 = \frac{L_4}{L} \end{gathered} \tag{14}$$

where ρ is the density of air, g the gravitational acceleration, and A_1 and A_3 are reference areas for the parachute and payload. Aerodynamic force coefficients are conventionally separated into normal force coefficient (C_N) and tangent force coefficient (C_T) in the parachute literature;

$$\begin{aligned} C_{N1} &= \frac{(F_{1x} + F_{1y})^{1/2}}{\frac{1}{2}\rho C_1^2A_1};\quad C_{T1} = \frac{-F_{1z}}{\frac{1}{2}\rho C_1^2A_1} \\ C_{N3} &= \frac{(F_{3x} + F_{3y})^{1/2}}{\frac{1}{2}\rho C_3^2A_3};\quad C_{T3} = \frac{-F_{3z}}{\frac{1}{2}\rho C_3^2A_3} \end{aligned} \tag{15}$$

The appropriate velocity magnitudes are shown in Fig. 2 to be C_1 for the parachute, and in Fig. 3 to be C_3 for the payload. Velocity magnitudes are expressed in dimensionless form as

$$\begin{aligned} c_1^2 &= u_1^2 + v_1^2 + w_1^2 \\ c_3^2 &= (u_3 + r_4q_3)^2 + (v_3 - r_4p_3)^2 + w_3^2 \end{aligned} \tag{16}$$

Also illustrated in Figs. 2 and 3 are angles of attack for the parachute and payload;

$$\begin{aligned} \alpha_1 &= \arctan[(u_1^2 + v_1^2)^{1/2}/w_1] \\ \alpha_3 &= \arctan\{[(u_3 + r_4q_3)^2 + (v_3 - r_4p_3)^2]^{1/2}/w_3\} \end{aligned} \tag{17}$$

Since the force coefficients are assumed to be functions only of instantaneous angles of attack, they can also be expressed solely in terms of velocities.

The dimensionless mass and moment of inertia parameters and the length ratios are defined in such a way that the equations of motion are made as simple as possible. They are not in convenient form for making a system parametric study or for efficiently using data available in the literature. More convenient forms will thus be defined.

Reference areas are taken as parachute and payload cross-sectional areas

$$A_1 = \pi D_1^2/4;\quad A_3 = \pi D_3^2/4 \tag{18}$$

where D_1 and D_3 are diameters. Parachute apparent mass and moment of inertia are put in dimensionless form by dividing by the mass and moment of inertia of a fluid sphere of appropriate reference diameter (see Ibrahim[10]).

$$B_m = 6m_a/\pi\rho D_1^3;\quad B_i = 60I_a/\pi\rho D_1^5 \tag{19}$$

It is often convenient in parametric studies to express moment of inertia as a simple function of mass and length:

$$I_1 = C_{I1}m_1D_1^2;\quad I_3 = C_{I3}m_3L_{3T}^2 \tag{20}$$

where C_{I1} and C_{I3} are constants and L_{3T} is total payload length. The following length ratios are likely to be found more convenient:

$$r_{21} = \frac{L_2}{L_1};\quad r_{3T} = \frac{L_3}{L_{3T}};\quad r_{4T} = \frac{L_4}{L_{3T}};\quad r_{D1} = \frac{D_1}{L_1};\quad r_{D3} = \frac{D_3}{L_{3T}} \tag{21}$$

Combining all of these new parameters with the descent Froude number, $Fr = C_0/(gL)^{1/2}$, the "simplifying" parameters of Eqs. (14) can be written in more convenient parameters as follows:

$$\begin{gathered} k_1 = \frac{C_{T0}Fr^2r_{1g}}{r_1} + \frac{4B_mr_{D1}}{3};\quad i_1 = \frac{C_{I1}C_{T0}Fr^2r_{1g}r_{D1}}{r_1} + \frac{2B_ir_{D1}^3}{15} \\ k_3 = \frac{C_{T0}Fr^2r_{3g}}{r_3r_A};\quad i_3 = \frac{C_{I3}C_{T0}Fr^2r_{3g}}{r_{3T}^2r_3r_A} \\ r_1 = (r_{D1}r_{3T}r_A^{1/2}/r_{D3} + r_{21} + 1)^{-1};\quad r_2 = r_{21}r_1 \\ r_3 = 1 - r_1 - r_2;\quad r_4 = r_{4T}r_3/r_{3T} \end{gathered} \tag{22}$$

Obviously, Froude number cannot be specified without indirectly specifying some physical characteristic of the system. By definition

$$Fr^2 = C_0^2/gL = 2m_{3g}/r_{3g}C_{T0}\rho A_1L \tag{23}$$

If an average payload density ρ_3 is defined for most reasonable payload shapes,

$$Fr^2 > 2\rho_3A_3L_3/r_{3g}C_{T0}\rho A_1L = (2r_Ar_3/r_{3g}C_{T0})(\rho_3/\rho) \tag{24}$$

Specifying Froude number is thus seen to be equivalent to specifying a payload to fluid density ratio. A reasonable minimum density ratio for Earth applications is found to be about 500. Accordingly, a minimum Froude number is defined as

$$Fr_m^2 = 1000\, r_Ar_3/r_{3g}C_{T0} \tag{25}$$

The ratio Fr/Fr_m is convenient for use in a parametric study.

Small-Disturbance Analysis

General Procedure

It is often desirable to dinstinguish between fundamentally different types of system behavior. To attempt to do so for a complicated system, using only numerical solutions of the equations of motion, can be a costly and frustrating task. An analysis of the stability of a given state is often more practical.

For example, usually a parachute and payload are required to descend in a steady glide rather than in some wildly oscillating manner. A stability analysis of the glide condition can be used to accomplish the desired result.

The mathematical techniques required to evaluate the stability of large systems of nonlinear differential equations are not generally available. Therefore, linear techniques are used and stability is considered with only small perturba-

tions about a reference state allowed. The linear stability analysis does not give a complete picture of system stability, but used properly, it is a valuable tool in predicting system behavior.

In the general procedure to be followed, the stability of a free system given an initial displacement is investigated. Either a portion, or all, of the general solution of the linear equations of motion can be investigated.

The extent to which the general solution is examined is determined by the amount of detail required in the stability analysis. If the maximum possible growth rate for an initial disturbance is sufficient information, the most positive real part of a characteristic polynomial root will do. If the stability of one or more specific modes is of interest, all the roots might be needed. It might even be desirable to evaluate the constants in the general solution, if the relative significance of certain modes is important.

A comparison of numerical solutions of the nonlinear equations of motion with general solutions of the linear equations of motion is also recommended. These comparisons have been found by experience to be extremely important when large systems of relatively unfamiliar equations are involved. The derivation of the general equations of motion is almost entirely dependent upon physical reasoning to ensure the correctness of the equations, within the intended assumptions. It can be very difficult with similar arguments to show that the stability analysis is consistent with the original equations of motion. Comparison of the general solution of the linear equations with a numerical solution of the original equations of motion for a number of test cases can give reasonable assurance that all intermediate steps, and hence the stability criteria, are correct.

Linear Equations

The first step in the small-disturbance analysis is to write the equations of motion in linear form. For the parachute and payload, a reference descent configuration is selected in which the entire system is axisymmetric. The small-disturbance analysis thus applies to a parachute and payload descending vertically.

To investigate the stability of the vertical descent condition, we assume small disturbances about a reference state defined by

$$u_1 = v_1 = u_3 = v_3 = 0,\ p_j = g_j = \psi_j = \theta_j = \phi_j = 0$$
$$w_1 = w_3 = 1 \tag{26}$$

Disturbance variables are denoted by primes, as follows:

$$u_1' = u_1;\quad v_1' = v_1;\quad u_3' = u_3;\quad v_3' = v_3;\quad p_j' = p_j$$
$$q_j' = q_j;\quad \psi_j' = \psi_j;\quad \theta_j' = \theta_j;\quad \phi_j' = \phi_j; \tag{27}$$
$$w_1' = w_1 - 1,\ w_3' = w_3 - 1$$

Force coefficient curves are approximated by straight lines near $\alpha = 0$ so that with $\alpha' = \alpha$,

$$C_{N1} = C_{N\alpha 1}\alpha_1';\quad C_{T1} = (C_{T1})_0;\quad C_{N3} = C_{N\alpha 3}\alpha_3'$$
$$C_{T3} = (C_{T3})_0;\quad C_{T0} = (C_{T1} + r_A C_{T3})_0 \tag{28}$$

Substituting Eqs. (27) and (28) into Eqs. (12) and neglecting squares and higher powers of disturbance variables, the linear equations of motion are obtained.

Equations in $u_1',\theta_1',u_3',\theta_3'$, and θ_2' separate to give

$$(D_* + G_1)u_1' + (D_* + G_2)\theta_1' - G_3\theta_2' = 0$$
$$(D_*^2 + G_4)\theta_1' - G_4\theta_2' = 0$$
$$(D_* + G_5)u_3' + (G_6 D_* + G_7)\theta_3' + G_8\theta_2' = 0 \tag{29}$$
$$G_9 u_3' + (D_*^2 + G_{10}D_* + G_{11})\theta_3' - G_{11}\theta_2' = 0$$
$$G_{12}u_1' + (G_{13}D_* + G_{12})\theta_1' - G_{12}u_3' +$$
$$(G_{14}D_* - G_{12})\theta_3' + D_*\theta_2' = 0$$

Equations in $v_1',\phi_1',v_3',\phi_3'$, and ϕ_2' also separate to give an equivalent set. The w_1' and w_3' equations form still another separate set, given by

$$(D_* + G_{15})w_3' = 0,\ D_* w_1' - D_* w_3' = 0 \tag{30}$$

The symbol D_* is the dimensionless time derivative, and the G coefficients are dimensionless groups defined as follows:

$$G_1 = \frac{C_{N\alpha 1}}{k_1 r_1};\quad G_2 = \frac{C_{T1}}{k_1 r_1};\quad G_3 = \frac{C_{T1} - r_{1_g}C_{T0}}{k_1 r_1}$$
$$G_4 = \frac{C_{T1} - r_{1_g}C_{T0}}{i_1 r_1^2};\quad G_5 = \frac{C_{N\alpha 3}}{k_3 r_3};\quad G_6 = 1 + \frac{C_{N\alpha 3} r_4}{k_3 r_3}$$
$$G_7 = \frac{C_{T3}}{k_3 r_3};\quad G_8 = \frac{C_{T1} - r_{1_g}C_{T0}}{k_3 r_3 r_A};\quad G_9 = \frac{C_{N\alpha 3} r_4}{i_3 r_3^3} \tag{31}$$
$$G_{10} = \frac{C_{N\alpha 3} r_4^2}{i_3 r_3^3};\quad G_{11} = \frac{C_{T1} - r_{1_g}C_{T0}}{i_3 r_3^2 r_A};\quad G_{15} = \frac{2C_{T0}}{k_1 r_1 + k_3 r_3 r_A}$$
$$G_{12} = \frac{1}{r_2};\quad G_{13} = \frac{r_1}{r_2};\quad G_{14} = \frac{r_3}{r_2}$$

The equivalence of the $\theta - u$ and the $\phi - v$ equations merely indicates the obvious result that a vertically descending parachute has no preferred plane of oscillation. Since the only root of Eqs. (30) is real and always positive, they are always stable.

General Solution

Equations (29) are linear ordinary differential equations with constant coefficients. Solutions must be of the form $e^{\lambda t_*}$, where λ is a constant. If the exponential forms of $u_1',\theta_1',u_3',\theta_3'$, and θ_2' are substituted, a set of equations identical with Eqs. (29) is obtained, with the operator D_* replaced by λ. By requiring the determinant of the coefficients to be zero, the characteristic polynomial in λ is obtained.

The set of five simultaneous equations gives a seventh-order characteristic polynomial, since two of the equations are second order. Expanding the determinant of coefficients and collecting terms with like powers of λ is a very tedious process for large systems. Even more tedious are the methods required to extract roots of the characteristic polynomial and evaluate constants in the general solution. All of these operations were therefore accomplished using a digital computer. An excellent means of extracting all polynomial roots is available as an IBM subroutine.[11] Subroutines which were used to form the characteristic polynomial, extract the most positive real part of a polynomial root, and evaluate general solution constants were prepared by Wolf.[12] With these computer programs, it is possible to rapidly generate and check stability information for any large set of linear ordinary differential equations of the type encountered in the present parachute stability study.

Sample Stability Analysis

The major emphasis in this study is on developing methods of describing the dynamic behavior of parachute and payload systems. A very brief stability analysis is presented so that the use of the methods might be illustrated more clearly.

Sample System

In this example a statically unstable payload is to be stabilized during its descent by using a parachute. The parachute must be kept approximately the same diameter as the payload so that the descent speed remains large.

The payload has the following dimensionless parameters:

$$C_{N\alpha 3} = 1.0;\quad C_{T3} = 0.5;\quad r_{4T} = 0.4$$
$$r_{3T} = 0.5;\quad r_{D3} = 0.33;\quad C_{I3} = 0.1 \tag{32}$$

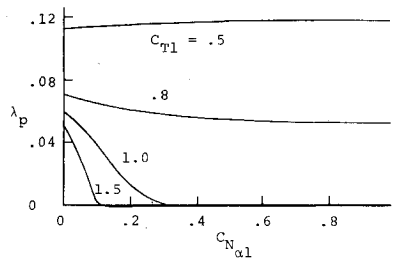

Fig. 5 Variation of λ_p with C_{T1}.

A parachute with the following dimensionless parameters is available:

$$C_{N\alpha 1} = 0.1; \quad C_{T1} = 1.0; \quad r_A = 1.0$$
$$B_m = 0.5; \quad B_i = 0.2; \quad r_{1g} = 0.05 \qquad (33)$$
$$r_{D1} = 0.5; \quad r_{21} = 5.0; \quad C_{I1} = 0.17$$

The analysis must determine if the parachute provides acceptable stability. If it does not, another parachute must be selected.

Stability Analysis

A recommended first step is to make certain that the stability analysis is consistent with the equations of motion.

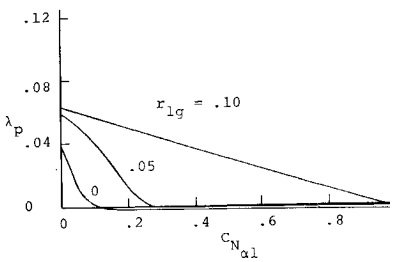

Fig. 6 Variation of λ_p with r_{1g}.

A comparison between numerical and general linear solutions shows (see Ref. 13) that the stability analysis and the equations of motion are consistent. An unstable divergence is also found to exist, so the parachute system must be modified. As a first step in determining how the system should be modified, the effects of varying available parachute parameters on λ_p is examined.

Figure 5 shows the effects of varying $C_{N\alpha 1}$ and C_{T1}. Clearly. $C_{N\alpha 1}$ should be increased as much as possible, and at least C_{T1} not decrease. The effect of parachute weight on system stability is dramatically illustrated in Fig. 6. Parachute weight must be kept at 5% or less of the total system weight. Figure 7 shows that the riser should be as short as possible. The system is shown to be more stable at high altitudes (large Froude numbers) in Fig. 8. All parameters are held constant at the values given in Eqs. (33) unless otherwise specified.

As a simplified modification, select a parachute with $C_{N\alpha 1}$ = 1.0, while keeping all other parameters the same. Even this drastic change may not make the system heavily damped, since it is shown to be only very slightly negative for $C_{N\alpha 1}$ as

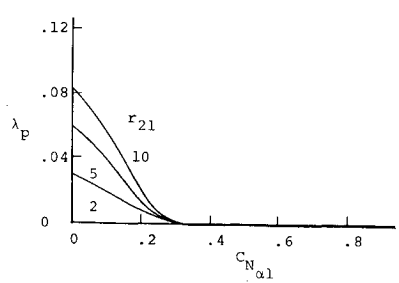

Fig. 7 Variation of λ_p with r_{21}.

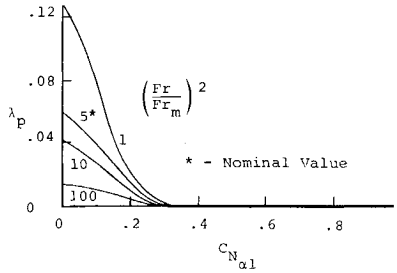

Fig. 8 Variation of λ_p with *Fr*.

large as 1.0. The significance of λ_p to the system behavior is easily determined by forming the characteristic polynomial, extracting all its roots, and evaluating the general solution constants for given initial conditions. The resulting roots [where $i = (-1)^{1/2}$] are

$$\lambda_{1,2} = -0.00004 \pm 1.74i \qquad \lambda_{3,4} = -0.0133 \pm 0.208i$$
$$\lambda_{5,6} = -0.0048 \pm 0.059i \qquad \lambda_7 = -0.0026 \qquad (34)$$

Given a one-degree pitch displacement, the solutions for θ_1 and θ_3 are

$$\theta_1 = e^{-0.000t_*}(-0.014\cos 1.74t_* + 0.000\sin 1.74t_*) + e^{-0.013t_*}(0.940\cos 0.208t_* + 0.041\sin 0.208t_*) + e^{-0.005t_*}(0.067\cos 0.059t_* + 0.066\sin 0.059t_*) + 0.006e^{-0.003t_*} \qquad (35a)$$

$$\theta_3 = e^{-0.000t_*}(-0.000\cos 1.74t_* + 0.000\sin 1.74t_*) + e^{-0.013t_*}(-0.889\cos 0.208t_* - 0.167\sin 0.208t_*) + e^{-0.005t_*}(1.88\cos 0.059t_* + 0.540\sin 0.059t_*) + 0.006e^{-0.003t_*} \qquad (35b)$$

The system is seen to be more heavily damped than the conservative parametric study using the most positive root indicated. Coefficients for the lightly damped modes ($\lambda_{1,2}$ and λ_7) are very small, whereas the more heavily damped modes ($\lambda_{3,4}$ and $\lambda_{5,6}$) have large coefficients.

Large-Disturbance Stability

As previously mentioned, a linear stability analysis does not give a complete picture of system stability. It does not necessarily give valid results for large amplitude motions.

Figure 9 shows the response of the "stable" system to 5° displacement; the initial pitch-up motion of the payload is turned back by the parachute; and although not shown, the oscillations eventually damp out. If the same system is displaced 10°, an uncontrolled divergence occurs. In both cases, force coefficients were approximated by

$$C_{N1} = 1.0\alpha_1 + 2.5\alpha_1^3 \qquad C_{T1} = 1.0 - 0.8\alpha_1^2$$
$$C_{N3} = 1.0\alpha_3 + 2.0\alpha_3^3 \qquad C_{T3} = 0.5 - 0.4\alpha_3^2 \qquad (36)$$

If the 5° displacement represents a reasonable upper limit, stability is assured. If not, some of the other parameters should be modified to increase system stability.

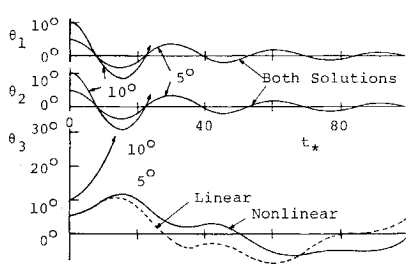

Fig. 9 Response of a stable system to large pitch displacements.

Also shown in Fig. 9 is the linear solution for a 5° pitch displacement. A considerable difference between the linear solution and the nonlinear solution for the payload pitch angle is apparent. For a similar one-degree displacement, the two solutions agree within ±0.04°.

Conclusions

Equations of motion that describe the three-dimensional motion of a nonrigid parachute and payload have been derived in a form which is convenient for numerical solution. A computer-aided small-disturbance stability analysis of the equations revealed that a relatively small parachute could be used to stabilize a statically unstable payload. Stability of the system was found to be improved by increasing parachute tangent force coefficient and normal force coefficient slope. Increasing riser length and parachute weight was seen to decrease system stability. The computer techniques developed allow a rapid stability analysis of large systems of linear ordinary differential equations of the type considered.

References

[1] Henn, H., "Descent Characteristics of Parachutes," R.A.E. Translation 233 of German Rept. ZWB/UM/6202, Oct. 1944, Royal Aircraft Establishment, Farnborough, England.

[2] Brown, W. D., *Parachutes*, Pitman and Sons Ltd., London, 1951.

[3] Lester, W. G. S., "A Note on the Theory of Parachute Stability," TN Mechanical Engineering 358, July 1962, Royal Aircraft Establishment, Farnborough, England.

[4] Heinrich, H. G. and Rust, L. W., "Dynamic Stability of a Parachute Point-Mass Load System," FDL-TDR-64-126, Air Force Flight Dynamics Lab., June 1965, Wright-Patterson Air Force Base, Ohio.

[5] Ludwig, R. and Heins, W., "Theoretical Studies of the Dynamic Stability of Parachutes," translated from the German by Faraday Translations, New York, Nov. 1964.

[6] White, F. M. and Wolf, D. F., "A Theory of Three-Dimensional Parachute Stability," *Journal of Aircraft*, Vol. 5, No. 1, Jan.-Feb. 1968, pp. 86–92.

[7] Heinrich, H. G. and Rust, L. W., "Dynamic Stability of a System Consisting of a Stable Parachute and an Unstable Load," AFFDL-TR-64-194, 1965, Air Force Flight Dynamics Lab., Wright-Patterson, Air Force Base, Ohio.

[8] Neustadt, M. et. al., "A Parachute Recovery System Dynamic Analysis," *Journal of Spacecraft and Rockets*, Vol. 4, No. 3, March 1967, pp. 321–326.

[9] Etkin, B., *Dynamics of Flight*, Wiley, New York, 1959.

[10] Ibrahim, S. K., "Experimental Determination of the Apparent Moment of Inertia of Parachutes," FDL-TDR-64-153, April 1965, Air Force Flight Dynamics Lab., Wright-Patterson Air Force Base, Ohio.

[11] "System/360 Scientific Subroutine Package," (360A-CM-03X) Version III, *Programmers Manual*, IBM H20-0205-3, 4th ed., 1968.

[12] Wolf, D. F., "The Dynamic Stability of Nonrigid Parachute and Payload System," Ph.D. thesis, 1968, Univ. of Rhode Island, Kingston, R.I.

AUGUST 1971 J. AIRCRAFT VOL. 8, NO. 8

Unsteady Airfoil Stall, Review and Extension

LARS E. ERICSSON* AND J. PETER READING†
Lockheed Missiles & Space Company, Sunnyvale, Calif.

A review of existing theoretical and experimental data has revealed that existing capabilities to predict full-scale unsteady airfoil stall are highly unsatisfactory. Existing theories can realistically only be applied to thin airfoil stall, and are completely inadequate in describing unsteady stall of the leading-edge or tailing-edge type, which comprise the stall types usually encountered both on helicopter rotors and compressor blades. The characteristic missing in present theories, and which completely dominates dynamic stall of the leading-edge and trailing-edge types, is the effect of pitch-rate-induced accelerated flow on the leeward side of a pitching airfoil. This flow acceleration produces a relief of the adversity of the pressure gradient, causing the observed delay of the stall and large overshoot of $C_{L_{max}}$. An analysis is presented that realistically describes unsteady airfoil stall in incompressible flow, including the accelerated flow effect on leading-edge and trailing-edge stall. It is found that quasi-steady theory, in which time history effects are lumped to one discrete past time event and the accelerated flow effect is represented by an equivalent time lag, can adequately describe the unsteady airfoil characteristics in the complete angle of attack range from substall into deep stall. Analytic predictions are found to agree well with dynamic experimental data. At very high frequencies, however, the agreement starts to deteriorate.

Nomenclature

AR = aspect ratio, $AR = b^2/S$
A/A_o = amplitude ratio, Eq. (2)
B/B_o = amplitude ratio, Eqs. (7–10)
b = wing span, m
C = general aerodynamic coefficient, Eqs. (1–3)
$c,\bar{c}$ = reference length, m: c = 2-dimensional chord length; $\bar{c} = S/b$, mean aerodynamic chord
f = frequency, cps
h = airfoil camber, m
L = lift, kg, coefficient $C_L = L/(\rho_\infty U_\infty^2/2)S$
l = lift, kg/m, coefficient $c_l = l/(\rho_\infty U_\infty^2/2)c$
M = Mach number
M_p = pitching moment, kg-m, $C_m = M_p/(\rho_\infty U_\infty^2/2)S\bar{c}$
m_p = pitching moment, kg-m/m, coefficient $c_m = m_p/(\rho_\infty U_\infty^2/2)c^2$
N = normal force, kg, coefficient $C_N = N/(\rho_\infty U_\infty^2/2)S$

Presented as Paper 70-77 at the AIAA 8th Aerospace Sciences Meeting, New York, January 19–21, 1970; submitted February 27, 1970, revision received November 19, 1970. The results were obtained in a study made for NASA Langley Research Center, Contract NAS 1-7999, under the direction of P. Hanson.

* Senior Staff Engineer. Associate Fellow AIAA.
† Research Specialist. Member AIAA.